Research in Astronomy and Astrophysics, 24:015012 (8pp), 2024 January https://doi.org/10.1088/1674-4527/ad0ded

Point-symmetry in SNR G1.9+0.3: A Supernova that Destroyed its Planetary Nebula Progenitor

Noam Soker
Department of Physics, Technion, Haifa, 3200003, Israel; soker@physics.technion.ac.il
Received 2023 September 29; revised 2023 November 11; accepted 2023 November 16; published 2023 December 19

Abstract

I analyze a new X-ray image of the youngest supernova remnant (SNR) in the Galaxy, which is the type Ia SNR G1.9+0.3, and reveal a very clear point-symmetrical structure. Since explosion models of type Ia supernovae (SNe Ia) do not form such morphologies, the point-symmetrical morphology must come from the circumstellar material (CSM) into which the ejecta expands. The large-scale point-symmetry that I identify and the known substantial deceleration of the ejecta of SNR G1.9+0.3 suggest a relatively massive CSM of $\gtrsim 1 M_{\odot}$. I argue that the most likely explanation is the explosion of this SN Ia into a planetary nebula. The scenario that predicts a large fraction of SN Ia inside PNe (SNIPs) is the core degenerate scenario. Other SN Ia scenarios might lead to only a very small fraction of SNIPs or none at all.

Key words: (stars:) supernovae: general – ISM: supernova remnants – (stars:) binaries (including multiple): close – (ISM:) planetary nebulae: general – stars: jets

1. Introduction

A point-symmetric morphology is composed of pairs of twin structural components on opposite sides of the center of the nebula. Such structures are clearly observed in many tens of planetary nebulae (PNe), as catalogs of PNe (and proto-PNe) reveal (e.g., Balick 1987; Chu et al. 1987; Schwarz et al. 1992; Corradi & Schwarz 1995; Manchado et al. 1996; Sahai & Trauger 1998; Sahai et al. 2011; Parker et al. 2016; Parker 2022). Many PNe are shaped by jets (e.g., Morris 1987; Soker 1990; Sahai & Trauger 1998), including point-symmetric morphologies (e.g., Sahai 2000; Sahai et al. 2007, 2011; Boffin et al. 2012). Many PNe and proto-PNe (e.g., Sahai et al. 2000, 2011), like the post-asymptotic giant branch (AGB) star IRAS 16594-4656 (Hrivnak et al. 2001), show that the point-symmetry is not always perfect. Namely, they might have some deviations from perfect point-symmetry. In particular, the two opposite clumps/lobes/arcs/filaments of a pair might have different structures, differ in brightness, be not exactly positioned at 180° to each other with respect to the center (bent-morphology) and have different distances from the center. As well, non-paired clumps might exist in the nebula.

PNe leave white dwarf (WD) remnants, in many cases a WD in a binary system. If the WD remnant explodes as a type Ia supernova (SN Ia) before the PN is dispersed into the interstellar medium (ISM), the PN might have an imprint on the morphology of the supernova (SN) remnant (SNR). An SN inside a PN is termed SNIP (e.g., Tsebrenko & Soker 2015a). Not all theoretical SN Ia and peculiar SN Ia scenarios allow for the formation of point-symmetric SNRs (for some recent reviews of the scenarios, but without reference to point-symmetry, see, e.g., Hoeflich 2017; Livio & Mazzali 2018; Soker 2018; Wang 2018; Jha et al. 2019; Ruiz-Lapuente 2019; Soker 2019; Ruiter 2020; Liu et al. 2023b).

The formation process of PNe, typically takes tens to thousands of years to form the dense shell, which is much longer than the dynamical time of the AGB progenitor, about one year. Also, the launching phase of the jets by a companion to the AGB progenitor is much longer than the dynamic time of the accretion disk that launches the jets. This allows for disk precession that launches opposite pairs of jets in varying directions. In SN Ia scenarios that involve a disk with bipolar explosion morphology (e.g., Perets et al. 2019; Zenati et al. 2023), the disk explosion time is not much longer, and even shorter, than the dynamical time of the disk. No disk precession is possible during the explosion. If an SNR Ia has a point-symmetry, it seems that it results from a point-symmetric circumstellar material (CSM).

Peculiar SNe Ia also might have peculiar morphologies, such as the unordered morphology of the peculiar SNR 3C 397 (e.g., Ohshiro et al. 2021) that might result from deflagration (Mehta et al. 2023). However, these are not expected to form point-symmetric morphologies. ISM magnetic fields might shape only one pair of twin structural features (e.g., Wu & Zhang 2019) and might play other roles in SNRs (e.g., Xiao et al. 2022). Velázquez et al. (2023) simulate non-spherical pre-explosion mass loss into a magnetized ISM. They find that when the pre-explosion wind is axisymmetric (rather than spherical) and its symmetry axis is inclined to the ISM magnetic field then the ears in the SNR might be bent.

However, point-symmetric clumps/filaments cannot be formed by this mechanism. Surrounding density inhomogeneities might also shape SNRs (e.g., Lu et al. 2021). However, these ISM effects cannot form point-symmetric structures. Zhang et al. (2023) simulated the shaping of SNR G1.9+0.3 with magnetic fields and ISM density gradients. They could form a pair of ears, but not a point-symmetry (which was not known then). Griffeth Stone et al. (2021) simulated SNR G1.9+0.3 as a highly non-spherical explosion into a uniform medium. This cannot form a point-symmetric structure. In a recent study, Villagran et al. (2023) conducted three-dimensional magneto-hydrodynamic simulations to reproduce the morphology and emission of SNR G1.9+0.3 by a non-spherical pre-explosion wind into a magnetized ISM. They also obtained an axisymmetrical morphology, but not a point-symmetry. Instabilities that develop in the ejecta-ISM interaction are not expected to form point-symmetric morphologies. Furthermore, Mandal et al. (2023) demonstrate with hydrodynamical models that the instabilities that develop as SNRs interact with an ambient medium have a characteristic peak in their power spectra that is relatively large, >10. This cannot account for a point-symmetric structure with only a few prominent pairs of opposite morphological features.

In this study, I identify a point-symmetric morphology in the newly released X-ray image of SNR G1.9+0.3 (Enokiya et al. 2023), a young SNR Ia that exploded around 1890–1900 (e.g., Carlton et al. 2011; Chakraborti et al. 2016; Borkowski et al. 2017; Pavlović 2017). I analyze the image in Section 3 and conclude that the most likely explanation is that this SNR was shaped by an SN Ia inside a PN, i.e., an SNIP.

Tsebrenko & Soker (2015b) already suggested that SNR G1.9+0.3 is an SNIP, and simulated its shaping. However, they did not refer to point-symmetry. The present analysis puts the SNIP suggestion on a very solid ground. To facilitate the analysis and discussion in Section 4, I start by considering the ability of different SN Ia scenarios to account for point-symmetric morphologies (Section 2).

2. Point-Symmetry in SN Ia Scenarios

In Table 1 I list SN Ia scenarios (first row) with some of their properties (second row). The properties are the number of stars in the system at the time of explosion $N_{\rm exp}$, the number of surviving stars after the explosion $N_{\rm sur}$, the mass of the exploding WD where $M_{\rm Ch}$ stands for near Chandrasekhar mass, and the morphology of the ejecta ($E_{\rm j}$) being spherical (S) or non-spherical (N). These properties refer to normal SNe Ia where the WD that explodes does not leave a remnant. The first two rows of the table are from a much larger table from Soker (2019) which compares the scenarios with each other and with observations. Scenarios where there is only one star at the explosion, $N_{\rm exp}=1$, are grouped into lonely WD scenarios, and might account for most, or even all, normal SNe Ia (Braudo & Soker 2023).

Here I add to Table 1 the third row that indicates whether the scenario might lead to a point-symmetric SNR, and describe below the scenarios only in their relation to a point-symmetric SNR.

The core degenerate (CD) scenario predicts that a large fraction of SNe Ia occurs inside PNe or PN remnants. These are termed SNIPs for SNe Ia Inside PNe. A PN remnant is an old PN shell that at the time of the explosion is mostly neutral and hence does not shine as a PN. The reason that the CD scenario predicts many SNIPs is that the core and the WD merge during or at the end of the common envelope evolution (CEE; e.g., Kashi & Soker 2011; Ilkov & Soker 2013; Aznar-Siguán et al. 2015), and might explode within several hundreds of thousands of years, which is the merger to explosion delay (MED) time. In Soker (2022) I estimated that the fraction of SNIPs among all normal SNe Ia in the Milky Way and the Magellanic clouds is $f_{\rm SNIP}({\rm local}) \simeq 70\%$–$80\%$, and its total fraction, including dwarfs and elliptical galaxies, is $f_{\rm SNIP}({\rm total}) \simeq 50\%$. I take two very recent studies of the CSM of SNe Ia, of Tycho's SNR (Kobashi et al. 2023) and of SN 2018evt (Wang et al. 2023), to actually support an SNIP scenario for these two SNe Ia. A point-symmetry in an SNR Ia is a natural possibility of the CD scenario when the progenitor PN of an SNIP has a point-symmetry. For a recent study of SNIPs in relation to SNR properties see Court et al. (2023).

In the double degenerate (DD) scenario (e.g., Iben & Tutukov 1984; Webbink 1984) without an MED time or with an MED time (e.g., Lorén-Aguilar et al. 2009; van Kerkwijk et al. 2010; Pakmor et al. 2013; Levanon et al. 2015; Levanon & Soker 2019; Neopane et al. 2022), there is a delay from the end of the CEE to the merger itself due to gravitational wave emission by the double WD system $t_{\rm GW}$. There are several channels of this scenario (e.g., Pakmor et al. 2011; Ablimit et al. 2016; Liu et al. 2016; Yungelson & Kuranov 2017; Perets et al. 2019; Zenati et al. 2019), with some recent interest in the violent merger channel (e.g., Maeda et al. 2023; Siebert et al. 2023a, 2023b; Axen & Nugent 2023; Kwok et al. 2023; Srivastav et al. 2023). In the DD scenario, the delay time from the end of the CEE to explosion is $t_{\rm CEED}=t_{\rm GW}$. In the DD-MED scenario, the time from the end of the CEE to the explosion itself also includes the MED time, and therefore $t_{\rm CEED}=t_{\rm GW}+t_{\rm MED}$ (see discussion in Soker 2022). The way to form a point-symmetric nebula is if the explosion takes place before the PN material is dispersed into the ISM, i.e., $t_{\rm CEED} \lesssim 10^6$ yr. However, due to the generally long gravitational-wave merger time $t_{\rm GW}$, this possibility is very rare.

In the different channels of the double detonation (DDet) scenario (e.g., Woosley & Weaver 1994; Livne & Arnett 1995; Papish et al. 2015; Shen et al. 2018a, 2018b; Ablimit 2021; Zingale et al. 2023) the explosion of a CO WD is triggered by the thermonuclear detonation of a helium layer on the WD.

Table 1
SN Ia Scenarios and their Ability to form a Point-symmetric SNR

Scenario[a]	Core Degenerate (CD)	Double Degenerate (DD)	Double Degenerate (DD-MED)	Double Detonation (DDet)	Single Degenerate (SD-MED)	WD-WD collision (WWC)
[N_{exp}, N_{sur}, M, Ej][a]	[1, 0, M_{Ch}, S]	[2, 0, sub-M_{Ch}, N]	[1, 0, M_{Ch}, S]	[2, 1, sub-M_{Ch}, N]	[2, 1, M_{Ch}, S]	[2, 0, sub-M_{Ch}, N]
Point-symmetry in the SNR	Expected in some SNIPs with point-symmetric PNe.	Very rare: A SNIP with point-symmetric PN.	Very rare: A SNIP with point-symmetric PN.	Extremely rare.	Possible: a symbiotic progenitor; Low-mass CSM.	Extremely rare; large-scale departures from an elliptical shape.

Notes.
[a] Scenarios for SN Ia by alphabetical order. MED: Merger to explosion delay time. It implies that the scenario has a delay time from merger or mass transfer to explosion. MED is an integral part of the CD scenario.
[b] N_{exp} is the number of stars in the system at the time of explosion; N_{sur} is the number of surviving stars in normal SNe Ia: $N_{sur} = 0$ if no companion survives the explosion while $N_{sur} = 1$ if a companion survives the explosion (in some peculiar SNe Ia the exploding WD is not destroyed and it also leaves a remnant); M_{Ch} indicates a (near) Chandrasekhar-mass explosion while sub-M_{Ch} indicates sub-Chandrasekhar mass explosion; Ej stands for the morphology of the ejecta, where S and N indicate whether the scenario might lead to spherical explosion or cannot, respectively.

This ignition takes place on a dynamic timescale and cannot lead to a point-symmetric morphology. Only if the explosion takes place within hundreds of thousands of years after the CEE of the progenitor binary system, i.e., $t_{\rm CEED} \lesssim 10^6$ yr, might this scenario lead to a point-symmetric remnant being an SNIP. My estimate (Soker 2019), based in part on the no detection of the surviving companions in SNRs (e.g., Li et al. 2019; Shields et al. 2022, 2023), is that the DDet scenario accounts for peculiar SNe Ia (e.g., Karthik Yadavalli et al. 2023; Liu et al. 2023; Padilla Gonzalez et al. 2023), but only rarely for normal SNe Ia. More rare will be normal SNe Ia through this channel that explode before the PNe are dispersed.

The single degenerate (SD) scenario (e.g., Whelan & Iben 1973; Han & Podsiadlowski 2004; Orio 2006; Wang et al. 2009; Meng & Podsiadlowski 2018; Cui et al. 2022) might in principle lead to a point-symmetric SNR if the CSM formed by the wind from a giant mass-donor has a point-symmetric morphology. This is basically an SN Ia inside a symbiotic nebula. Symbiotic progenitors of SNe Ia are very rare (e.g., Laversveiler & Gonçalves 2023). There are two main differences between symbiotic progenitors and SNIPs: (1) In the case of an SD scenario, the expectation is for the presence of a red giant branch star or an AGB star in the SNR. (2) The CSM mass is much smaller than in an SNIP. The large deceleration of the ejecta of SNR G1.9+0.3 makes this scenario less likely (Section 4).

The very rare (e.g., Toonen et al. 2018; Hallakoun & Maoz 2019; Hamers & Thompson 2019; Grishin & Perets 2022) WD–WD collision (WWC) scenario, where two unbound WDs collide with each other (e.g., Raskin et al. 2009; Rosswog et al. 2009; Kushnir et al. 2013; Aznar-Siguán et al. 2014; Glanz et al. 2023) does not predict a point-symmetric SNR as I study here. The collision of two equal mass WDs can lead to a large-scale bipolar structure in case of a head-on collision (e.g., Hawley et al. 2012), or to a large-scale point-symmetric ejecta with a very large departure from a large-scale elliptical shape (e.g., Glanz et al. 2023). The demand for equal-mass WDs in a scenario that is extremely rare to start with and the large departures from an elliptical shape make this scenario unlikely to explain the point-symmetric morphology of SNR G1.9+0.3 that I study here.

The overall conclusion from this discussion is that the most likely explanation for a point-symmetric SNR Ia morphology is an SNIP. The scenario that statistically has the largest fraction of SNIPs is the CD scenario. I return to this point in Section 4.

3. Point-symmetry in SNR G1.9+0.3

In their recent study Enokiya et al. (2023) combined 26 individual X-ray observations of SNR G1.9+0.3 from 2007 to 2015 in the energy range of 0.5–7 keV. They obtained a detailed X-ray image that reveals detailed structures (previous X-ray studies include, e.g., Reynolds et al. 2008, 2009; Borkowski et al. 2010; Carlton et al. 2011; Borkowski et al. 2013, 2014; Zoglauer et al. 2015; Borkowski et al. 2017). In addition, they present contours of molecular emission which they use to identify molecular clouds. In this study, I refer only to the X-ray morphology. I do not consider abundance or molecular clouds.

Borkowski et al. (2017) present an X-ray image very similar to that by Enokiya et al. (2023). The new one allows a better analysis of the point-symmetry. Borkowski et al. (2017) present the proper expansion velocities on the plane of the sky and find two strong properties. The first is that the arcs that are closer to the center, in the north and south directions, expand much more slowly than the ears. Following Tsebrenko & Soker (2015b), I take the arcs to be part of the equatorial structure and the ears to be along the polar directions of the PN into which SNR G1.9 +0.3 exploded. The second property that Borkowski et al. (2017) find is that many regions expand not exactly along radial directions. I attribute these properties of slowly expanding arcs and non-radial expansion directions to the interaction of the ejecta with a non-homogeneous PN shell (the CSM). For such an influence of the CSM on the ejecta, it should be massive, $\gtrsim 1 M_\odot$, almost ruling out the SD scenario (see Section 3) where the CSM is due to an AGB wind. Borkowski et al. (2014) find that the relative proper expansion rate (percentage per year) of the outer parts of the polar regions (that include the ears) is lower than that of the inner regions. This indicates substantial deceleration of the outer parts of the ejecta along and near the polar directions, again, requiring a relatively massive CSM. Some parts in the nebula have expansion velocities that are about half, and even less, than other parts. To decelerate the velocity to half its initial value requires, in a momentum-conserving interaction, a CSM mass that is about equal to the mass of the ejecta. In an energy-conserving case, there is a need for a larger CSM mass. Overall, the CSM mass should be about equal to the decelerated ejecta mass and more. Since a large fraction of the $\simeq 1.4 M_\odot$ ejecta is decelerated, I estimate the CSM mas to be $\gtrsim 1 M_\odot$.

In Figure 1 I take an image from Enokiya et al. (2023) to which I added the marks of the two ears and added double-headed arrows. I identify six pairs of clumps, marked with double-headed arrows DHA-a to DHA-f, and one tentative, DHA-τ, that together form a point-symmetric structure around the center. I analyze later the two opposite arcs that the two white double-headed arrows point at and reveal a bent point-symmetry.

DHA-e and DHA-f define two opposite arcs at about the same distance from the center. This is the most symmetric point-symmetric component because the two twin arcs (colored green) are at about the same distance from the center and about the same size. DHA-a points at a clump in the upper part of the image, and at a clump in the bottom that is at about the same distance from the center. DHA-b points to two clumps along

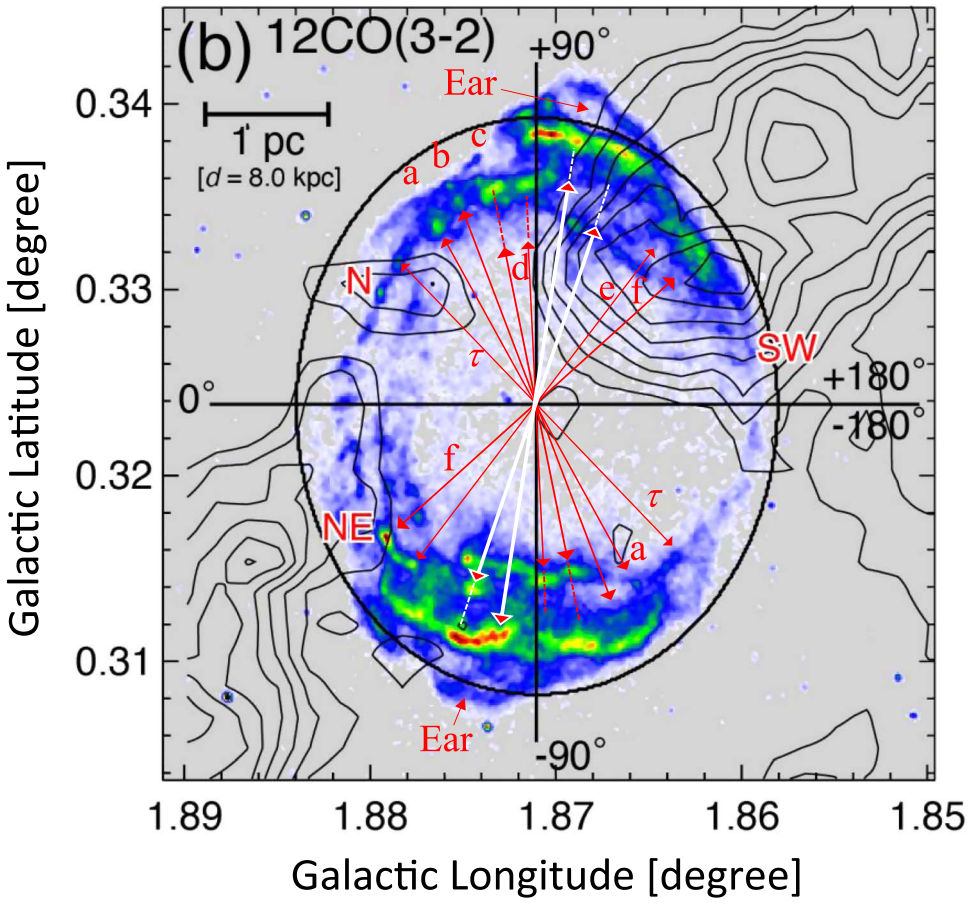

Figure 1. An X-ray image with CO contours from Enokiya et al. (2023). The ellipse and coordinate lines are in the original image. My additions are the double-headed arrows with dashed-line continuations and the marks of the two ears. The center of each double-headed arrow is at the center of the image (where the two black lines cross each other). The six red double-headed arrows DHA-a to DHA-f point at what I interpret as twin clumps of a point-symmetric structure, with DHA-τ indicating a tentative pair due to the small and relatively faint clumps. The two white double-headed arrows signify that although each double-headed arrow points at two opposite clumps to the center, I do not consider them as point-symmetry twins. My interpretation of the point-symmetric structure of these clumps is in Figure 2.

the arrow direction on the upper part of the image, and at a faint green filament at the bottom. Along the direction of DHA-b further away from the faint filament at the bottom, i.e., at the outer part of the SNR, there is the bright arc that DHA-a approximately defines as its bright edge. DHA-c and DHA-d point at two twin clumps, but those at the upper part of the image are at a larger distance from the center than the two clumps at the bottom. DHA-d points at a clump in the upper part at the same distance as the bright clump (yellow-red) on the bottom outer arc, as the red-dashed continuation lines show. In addition to these six pairs, there is a tentative pair marked by DHA-τ. It is tentative because the two opposite clumps are smaller and fainter than the others.

Overall, the point-symmetric structure that the red double-headed arrows define is not perfect although very strong. Considering that the ejecta of this SNR is strongly decelerated, namely interacting with a CSM, it is expected that the point-symmetry is not perfect. This is the situation also with tens of PNe (see catalogs listed in Section 1). The asymmetrical interaction of the ejecta of SNR G1.9+0.3 with the CSM and ISM is evident from the radio images of SNR G1.9+0.3 that present non-uniform brightness and large deviations from spherical symmetry (e.g., Green et al. 2008; Gómez & Rodríguez 2009; Borkowski et al. 2010; De Horta et al. 2014; Borkowski et al. 2017; Luken et al. 2020; Enokiya et al. 2023). As said, this interaction is related also to the non-radial velocity of many parts in this SNR that Borkowski et al. (2017) pointed out.

I turn to consider the clumps that the white arrows point at in Figure 1. Motivated by the bent-morphology of $\approx$10% of PNe (Soker & Hadar 2002) I consider the same for the two ears of SNR G1.9+0.3 and the bright arc at the base of each ear. In the bent-morphology, the symmetry axis is bent through the center, i.e., the angle between the directions to the two opposite

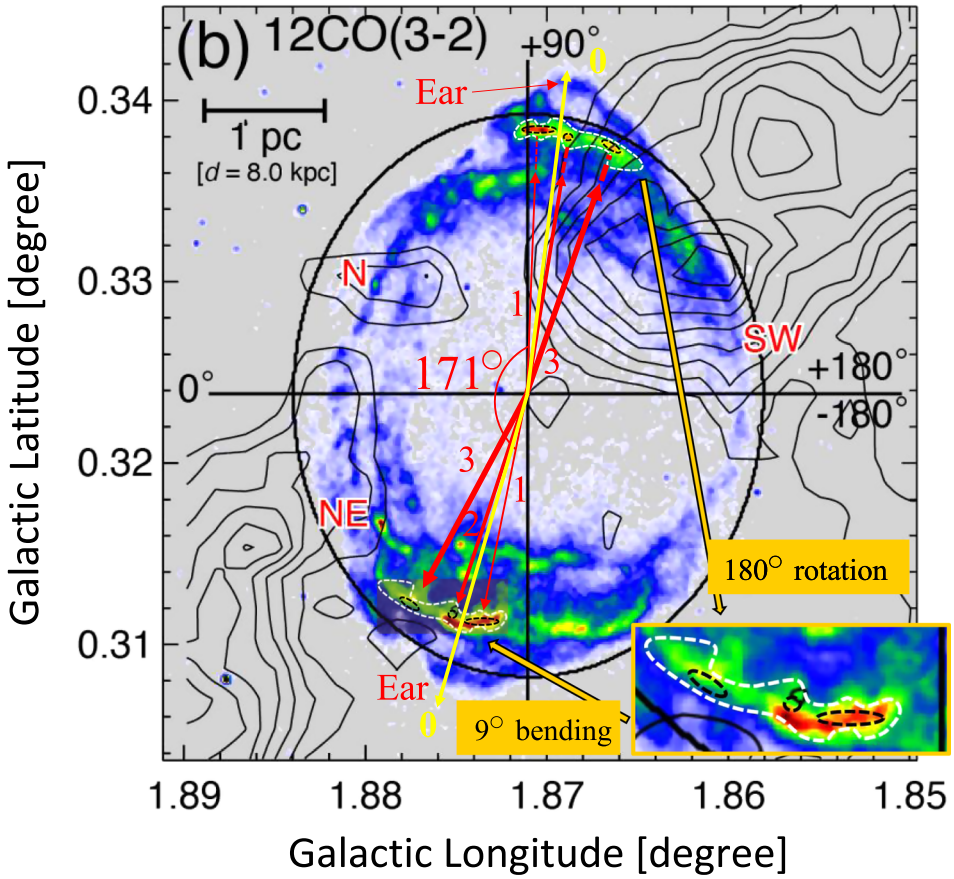

Figure 2. Presentation of the bent point-symmetrical structure of SNR G1.9+0.3. The original X-ray image from Enokiya et al. (2023) is the same as in Figure 1. I marked the arc at the base of the upper (western) ear with a dashed-white line and its three peaks (yellow-red) with three dashed-black lines. DHA-1 to DHA-3 point at these clumps. I copied and rotated this structure around itself by 180° and matched it to the arc at the base of the bottom (eastern) ear. The inset on the lower right enlarges this region. There is a 9° bent point-symmetry of the two ears (DHA-0) and of the two base arcs (DHA-1 to DHA-3).

clumps/lobes/arc/filaments is <180°. In other words, the two opposite structures are displaced in the same direction perpendicular to the symmetry axis.

In Figure 2 I present the 9°-bent morphological feature of the ears of SNR G1.9+0.3. I construct it as follows. I circle the green-colored arc at the base of the upper (western) ear with a dashed-white line. I also circle by dashed-black lines the three red-yellow peaks inside this arc. I then copy this entire structure to the bottom (eastern) ear and rotate it around itself by 180° and displace it to match the arc at the base of the eastern ear. I enlarge the bottom (eastern) arc in the inset on the lower-right of Figure 2. I find that the best match of the two twin arcs is when the angle through the center is 171° instead of 180° as marked on Figure 2. I also added to the figure two yellow arrows at 171° to each other, each arrow through the tip of an ear. The four bent double-headed arrows in Figure 2 define the 9°-bent point-symmetrical morphological component of SNR G1.9+0.3.

Based on the classification of bent-morphology PNe, I consider the value of the 9° bend to be significant. For example, the PN NGC 6826 is classified to have a bent-morphology (Soker & Hadar 2002) although its bending angle is only 7°. The features on which I base the bent-morphology are bright, namely, two opposite tangential arcs (marked by dashed-white lines), with bright clumps inside each of the two arcs. Overall, I consider the bent-morphology to be observationally significant.

I note that Chiotellis et al. (2021) consider the ears to form in the equatorial plane. This cannot account for a point-symmetry near the ears as I find here. The point-symmetry that I identify in SNR G1.9+0.3 shows, in very strong terms, that the ears are along the polar directions (e.g., Tsebrenko & Soker 2013, 2015b) and not in the equatorial plane. Most likely jets shaped the point-symmetrical structure of SNR G1.9 +0.3 through their shaping of a PN shell. This brings me to discuss this SNR as an SNIP.

4. Discussion and Summary

In this short study I analyzed a new X-ray image of SNR G1.9+0.3 (Enokiya et al. 2023) and revealed a clear point-symmetric morphology. I now discuss the possible implications on the SN Ia scenario that best explains the youngest SN Ia in the Galaxy.

Figures 1 and 2 present the point-symmetric structural features (the point-symmetric morphology) that I identify in SNR G1.9+0.3. In addition to the ears, there are several pairs of clumps and arcs that I identify. In several pairs and one tentative pair the two twin clumps/arcs are in opposite directions, sometimes at somewhat different distances from the center (Figure 1). The ears and the arc at the base of each ear form a bent point-symmetrical structure, as marked by DHA-0 to DHA-3 on Figure 2.

The point-symmetric structure that I identify in SNR G1.9 +0.3 is composed of opposite pairs of clumps/arcs/ears that have different directions (the directions of the double-headed arrows). Opposite pairs of jets with varying axis directions, like due to precession, form such structures in a rich variety of astrophysical systems, e.g., from PNe to jet-shaped bubbles in clusters of galaxies. Since explosion models of SNe Ia do not have jets with varying directions (Section 2), the most likely explanation is that the ejecta of SNR G1.9+0.3 expands into a point-symmetric CSM. The substantial deceleration of the ejecta of SNR G1.9+0.3 requires a massive CSM, which is more likely to be a PN that was expelled during a CEE in the CD scenario than an AGB wind in the SD scenario (Section 2). Although the DD and the DDet scenarios might also occur shortly after the CEE, the probability for that is much lower than that in the CD scenario (Section 2). Also, based on the upper bound of its ^{44}Ti abundance, Kosakowski et al. (2023) argue that SNR G1.9+0.3 is most consistent with a near-$M_{\rm Ch}$ progenitor. The CD scenario is compatible with that finding.

The interaction of the ejecta with the PN started some tens of years ago at a radius of $\lesssim 1$ pc. PNe can have such sizes, e.g., the PN IPHASX J055226.2+323724 in the open cluster M37 (Fragkou et al. 2022) with an age of $\simeq 10^5$ yr (Fragkou et al. 2022; Werner et al. 2023). Therefore, the explosion could have taken place while the PN was still shining, rather than exploding into an old post-PN shell.

I conclude that the most likely explanation for the point-symmetry of SNR G1.9+0.3 is an SNIP where the explosion took place into a PN (rather than a remnant of a PN). The explosion destroyed the WD, hence destroying the PN.

Acknowledgments

I thank an anonymous referee for helpful comments. This research was supported by a grant from the Israel Science Foundation (769/20).

ORCID iDs

Noam Soker https://orcid.org/0000-0003-0375-8987

References

Ablimit, I. 2021, PASP, 133, 074201
Ablimit, I., Maeda, K., & Li, X.-D. 2016, ApJ, 826, 53
Axen, M. F., & Nugent, P. 2023, ApJ, 953, 13
Aznar-Siguán, G., García-Berro, E., Lorén-Aguilar, P., Soker, N., & Kashi, A. 2015, MNRAS, 450, 2948
Aznar-Siguán, G., García-Berro, E., Magnien, M., & Lorén-Aguilar, P. 2014, MNRAS, 443, 2372
Balick, B. 1987, AJ, 94, 671
Boffin, H. M. J., Miszalski, B., Rauch, T., et al. 2012, Science, 338, 773
Borkowski, K. J., Gwynne, P., Reynolds, S. P., et al. 2017, ApJL, 837, L7
Borkowski, K. J., Reynolds, S. P., Green, D. A., et al. 2010, ApJL, 724, L161
Borkowski, K. J., Reynolds, S. P., Green, D. A., et al. 2014, ApJL, 790, L18
Borkowski, K. J., Reynolds, S. P., Hwang, U., et al. 2013, ApJL, 771, L9
Braudo, J., & Soker, N. 2023, arXiv:2310.16554
Carlton, A. K., Borkowski, K. J., Reynolds, S. P., et al. 2011, ApJL, 737, L22
Chakraborti, S., Childs, F., & Soderberg, A. 2016, ApJ, 819, 37
Chiotellis, A., Boumis, P., & Spetsieri, Z. T. 2021, MNRAS, 502, 176
Chu, Y.-H., Jacoby, G. H., & Arendt, R. 1987, ApJS, 64, 529
Corradi, R. L. M., & Schwarz, H. E. 1995, A&A, 293, 871
Court, T., Badenes, C., Lee, S.-H., et al. 2023, arXiv:2309.00572
Cui, Y., Meng, X., Podsiadlowski, P., & Song, R. 2022, A&A, 667, A154
De Horta, A. Y., Filipovic, M. D., Crawford, E. J., et al. 2014, SerAJ, 189, 41
Enokiya, R., Sano, H., Filipović, M. D., et al. 2023, PASJ..tmp., 75, 970
Fragkou, V., Parker, Q. A., Zijlstra, A. A., et al. 2022, ApJL, 935, L35
Glanz, H., Perets, H. B., & Pakmor, R. 2023, arXiv:2309.03300
Gómez, Y., & Rodríguez, L. F. 2009, RMxAA, 45, 91
Green, D. A., Reynolds, S. P., Borkowski, K. J., et al. 2008, MNRAS, 387, L54
Griffeth Stone, A., Johnson, H. T., Blondin, J. M., et al. 2021, ApJ, 923, 233
Grishin, E., & Perets, H. B. 2022, MNRAS, 512, 4993
Hallakoun, N., & Maoz, D. 2019, MNRAS, 490, 657
Hamers, A. S., & Thompson, T. A. 2019, ApJ, 882, 24
Han, Z., & Podsiadlowski, P. 2004, MNRAS, 350, 1301
Hawley, W. P., Athanassiadou, T., & Timmes, F. X. 2012, ApJ, 759, 39
Hoeflich, P. 2017, Handbook of Supernovae, Vol. 2017 (Berlin: Springer), 1151
Hrivnak, B. J., Kwok, S., & Su, K. Y. L. 2001, AJ, 121, 2775
Iben, I., Jr, & Tutukov, A. V. 1984, ApJS, 54, 335
Ilkov, M., & Soker, N. 2013, MNRAS, 428, 579
Jha, S. W., Maguire, K., & Sullivan, M. 2019, NatAs, 3, 706
Karthik Yadavalli, S., Villar, V. A., Izzo, L., et al. 2023, arXiv:2308.12991
Kashi, A., & Soker, N. 2011, MNRAS, 417, 1466
Kobashi, R., Lee, S.-H., Tanaka, T., & Maeda, K. 2023, arXiv:2310.14841
Kosakowski, D., Ugalino, M. I., Fisher, R., et al. 2023, MNRAS, 519, L74
Kushnir, D., Katz, B., Dong, S., Livne, E., & Fernández, R. 2013, ApJL, 778, L37
Kwok, L. A., Siebert, M. R., Johansson, J., et al. 2023, arXiv:2308.12450
Laversveiler, M., & Gonçalves, D. R. 2023, arXiv:2309.04466
Levanon, N., & Soker, N. 2019, ApJL, 872, L7
Levanon, N., Soker, N., & García-Berro, E. 2015, MNRAS, 447, 2803
Li, C.-J., Kerzendorf, W. E., Chu, Y.-H., et al. 2019, ApJ, 886, 99
Liu, C., Miller, A. A., Boos, S. J., et al. 2023, arXiv:2308.06319
Liu, D.-D., Wang, B., Podsiadlowski, P., & Han, Z. 2016, MNRAS, 461, 3653
Liu, Z.-W., Röpke, F. K., & Han, Z. 2023b, RAA, 23, 082001
Livio, M., & Mazzali, P. 2018, PhR, 736, 1
Livne, E., & Arnett, D. 1995, ApJ, 452, 62
Lorén-Aguilar, P., Isern, J., & García-Berro, E. 2009, A&A, 500, 1193
Lu, C.-Y., Yan, J.-W., Wen, L., & Fang, J. 2021, RAA, 21, 033
Luken, K. J., Filipović, M. D., Maxted, N. I., et al. 2020, MNRAS, 492, 2606
Maeda, K., Jiang, J.-an., Doi, M., Kawabata, M., & Shigeyama, T. 2023, MNRAS, 521, 1897

Manchado, A., Guerrero, M. A., Stanghellini, L., & Serra-Ricart, M. 1996, in The IAC Morphological Catalog of Northern Galactic Planetary Nebulae, ed. S. R. Pottasch (La Laguna: Instituto de Astrofisica de Canarias (IAC))
Mandal, S., Duffell, P. C., Polin, A., & Milisavljevic, D. 2023, ApJ, 956, 130
Mehta, V., Sullivan, J., Fisher, R., Ohshiro, Y., & Yamaguchi, H. 2023, in 242nd Meeting of the American Astronomical Society, 55 (Albuquerque, NM: AAS)
Meng, X., & Podsiadlowski, P. 2018, ApJ, 861, 127
Morris, M. 1987, PASP, 99, 1115
Neopane, S., Bhargava, K., Fisher, R., et al. 2022, ApJ, 925, 92
Ohshiro, Y., Yamaguchi, H., Leung, S.-C., et al. 2021, ApJL, 913, L34
Orio, M. 2006, ApJ, 643, 844
Padilla Gonzalez, E., Howell, D. A., Terreran, G., et al. 2023, arXiv:2308.06334
Pakmor, R., Hachinger, S., Röpke, F. K., & Hillebrandt, W. 2011, A&A, 528, A117
Pakmor, R., Kromer, M., Taubenberger, S., & Springel, V. 2013, ApJL, 770, L8
Papish, O., Soker, N., García-Berro, E., & Aznar-Siguán, G. 2015, MNRAS, 449, 942
Parker, Q. A. 2022, FrASS, 9, 895287
Parker, Q. A., Bojičić, I. S., & Frew, D. J. 2016, JPhCS, 728, 032008
Pavlović, M. Z. 2017, MNRAS, 468, 1616
Perets, H. B., Zenati, Y., Toonen, S., & Bobrick, A. 2019, arXiv:1910.07532
Raskin, C., Timmes, F. X., Scannapieco, E., Diehl, S., & Fryer, C. 2009, MNRAS, 399, L156
Reynolds, S. P., Borkowski, K. J., Green, D. A., et al. 2008, ApJL, 680, L41
Reynolds, S. P., Borkowski, K. J., Green, D. A., et al. 2009, ApJL, 695, L149
Rosswog, S., Kasen, D., Guillochon, J., & Ramirez-Ruiz, E. 2009, ApJL, 705, L128
Ruiter, A. J. 2020, IAUS, 357, 1
Ruiz-Lapuente, P. 2019, NewAR, 85, 101523
Sahai, R. 2000, ApJL, 537, L43
Sahai, R., Bujarrabal, V., Castro-Carrizo, A., & Zijlstra, A. 2000, A&A, 360, L9
Sahai, R., Morris, M., Sánchez Contreras, C., & Claussen, M. 2007, AJ, 134, 2200
Sahai, R., Morris, M. R., & Villar, G. G. 2011, AJ, 141, 134
Sahai, R., & Trauger, J. T. 1998, AJ, 116, 1357
Schwarz, H. E., Corradi, R. L. M., & Melnick, J. 1992, A&AS, 96, 23
Shen, K. J., Boubert, D., Gänsicke, B. T., et al. 2018a, ApJ, 865, 15
Shen, K. J., Kasen, D., Miles, B. J., & Townsley, D. M. 2018b, ApJ, 854, 52
Shields, J. V., Arunachalam, P., Kerzendorf, W., et al. 2023, ApJL, 950, L10
Shields, J. V., Kerzendorf, W., Hosek, M. W., et al. 2022, ApJL, 933, L31
Siebert, M. R., Foley, R. J., Zenati, Y., et al. 2023a, arXiv:2306.11788
Siebert, M. R., Kwok, L. A., Johansson, J., et al. 2023b, arXiv:2308.12449
Soker, N. 1990, AJ, 99, 1869
Soker, N. 2018, SCPMA, 61, 49502
Soker, N. 2019, NewAR, 87, 101535
Soker, N. 2022, RAA, 22, 035025
Soker, N., & Hadar, R. 2002, MNRAS, 331, 731
Srivastav, S., Smartt, S. J., Huber, M. E., et al. 2023, ApJL, 943, L20
Toonen, S., Perets, H. B., & Hamers, A. S. 2018, A&A, 610, A22
Tsebrenko, D., & Soker, N. 2013, MNRAS, 435, 320
Tsebrenko, D., & Soker, N. 2015a, MNRAS, 447, 2568
Tsebrenko, D., & Soker, N. 2015b, MNRAS, 450, 1399
van Kerkwijk, M. H., Chang, P., & Justham, S. 2010, ApJL, 722, L157
Velázquez, P. F., Meyer, D. M.-A., Chiotellis, A., et al. 2023, MNRAS, 519, 5358
Villagran, M. A., Gómez, D. O., Velázquez, P. F., et al. 2023, MNRAS, 527, 1601
Wang, B. 2018, RAA, 18, 049
Wang, B., Meng, X., Chen, X., & Han, Z. 2009, MNRAS, 395, 847
Wang, L., Hu, M., Wang, L., et al. 2023, arXiv:2310.14874
Webbink, R. F. 1984, ApJ, 277, 355
Werner, K., Reindl, N., Raddi, R., et al. 2023, A&A, 678, A89
Whelan, J., & Iben Jr, I. 1973, ApJ, 186, 1007
Woosley, S. E., & Weaver, T. A. 1994, ApJ, 423, 371
Wu, D., & Zhang, M.-F. 2019, RAA, 19, 124
Xiao, L., Zhu, M., Sun, X.-H., Jiang, P., & Sun, C. 2022, RAA, 22, 035003
Yungelson, L. R., & Kuranov, A. G. 2017, MNRAS, 464, 1607
Zenati, Y., Perets, H. B., Dessart, L., et al. 2023, ApJ, 944, 22
Zenati, Y., Toonen, S., & Perets, H. B. 2019, MNRAS, 482, 1135
Zhang, S., Tian, W., Zhang, M., Zhu, H., & Cui, X. 2023, ApJ, 942, 94
Zingale, M., Chen, Z., Rasmussen, M., et al. 2023, arXiv:2309.01802
Zoglauer, A., Reynolds, S. P., An, H., et al. 2015, ApJ, 798, 98